Wavelet-Transform-Based Data-Length-Variation Technique for Fast Heart Rate Detection Using 5.8-GHz CW Doppler Radar

Meiyu Li and Jenshan Lin, *Fellow, IEEE*

***Abstract*— The fast detection of heart rate (HR) is challenging when using the noncontact continuous-wave (CW) Doppler radar. Applying the Fourier transform (FT) to the baseband signal analysis, the accuracy is degraded due to the insufficient frequency resolution if using less than 5-s time window to realize fast detection. Moreover, respiratory harmonic peak might be incorrectly picked as the heartbeat signal if its magnitude is larger than the heartbeat peak in frequency spectrum. In this paper, a wavelet-transform-based data-length-variation technique is proposed to realize the fast detection of HR. With this technique, HR can be extracted with 3–5-s data length, and the respiratory harmonics can be distinguished from heartbeat signals, because the frequency of wavelet harmonic is not as tolerant of the change of the data length as heartbeat in the wavelet frequency spectrum. The algorithm is verified by simulation using numerical computing tool and demonstrated by human tests utilizing a 5.8-GHz CW Doppler radar platform. Compared to the traditional frequency domain method using FT, the proposed technique reduces the average error of HR from 26.7% to 3.5% using 3–5-s length of data varied in the range of ±0.5 s.**

***Index Terms*— Data-length-variation, Doppler radar vital signs detection, heart rate (HR), noncontact continuous wave (CW), wavelet transforms (WTs).**

I. Introduction

SINCE the first set of reports on noncontact measurement of human's and animals' respiratory and heartbeat movements proposed in [1]–[3], tremendous efforts have been devoted to apply this technique to healthcare, such as overnight monitoring of human vital signs [4], life detection for finding human subjects trapped in earthquake rubble [5], animal health care [6], [7], and general vital sign detection [8]–[11]. Among numerous noncontact vital sign detection techniques, using the microwave Doppler radar phase modulation effect is one of the most popular approaches. However, harmonics issue and heart rate (HR) acquisition speed are the challenges when applying continuous-wave (CW) Doppler radar to the fast and accurate vital signs detection. This motivates the study of the work in this paper.

Manuscript received January 1, 2017; revised May 2, 2017 and June 10, 2017; accepted June 21, 2017. *(Corresponding author: Meiyu Li.)*

The authors are with the Department of Electrical and Computer Engineering, University of Florida, Gainesville, FL 32611 USA (e-mail: meiyuli@ufl.edu; jenshan@ieee.org).

Color versions of one or more of the figures in this paper are available online at http://ieeexplore.ieee.org.

Digital Object Identifier 10.1109/TMTT.2017.2730182

There are three sources of harmonics in CW Doppler radar detection technique. The first is the nonlinearity of the radar transceiver circuits. This can be relieved by the proper design of the radar transceiver to ensure the linearity. The second is nonsinusoidal chest-wall movements induced by respirations. The third is the nonlinear phase demodulation employed to the baseband signal processing. Doppler radar measures the chest-wall movements, which are a combination of movements due to heartbeat and respiration. The displacement due to heartbeat is typically much smaller than that due to respiration [12]. So the strength of the respiratory harmonics is comparable to or even larger than that of a heartbeat. In frequency domain, one of the respiratory harmonic is very likely to be incorrectly picked as a heartbeat signal, which degrades the accuracy of HR extraction. Arctangent demodulation [13] does not have this harmonic interference issue, but it is sensitive to the dc offset, thus requiring complicated calibration. Complex signal demodulation (CSD) [14] does not require the calibration, but it generates harmonics. A respiratory harmonics cancellation method [15] was developed for CSD, but it required a long time window to achieve a sufficient frequency spectrum resolution to accurately locate the tones and cancel them. Respiratory harmonics can be predicted by time-window-variation technique [16] proposed afterward. The novel state-space-based algorithm [17] does not produce harmonics, and thus, it is able to accurately extract the HR.

The second challenge of vital sign detection using CW Doppler radar is how to realize fast acquisition of HR for real-time monitoring. Many applications, such as measuring vital signs of incoming patients at the registration desk in a hospital and the monitoring of HR variability which may indicate congestive heart failure or susceptibility to sudden infant death syndrome, require fast acquisition of HR, typically less than 5 s [16]. Most current techniques analyzing in frequency domain using the Fourier transform (FT)-based algorithm require a time-window length longer than 10 s [14], [15], [18] in order to achieve a spectrum resolution better than 0.1 Hz, which corresponds to six beats per minute (bpm). The most recently reported FT-based time-window-variation technique was able to extract HR by using 2–5-s short-period time window [16].

All frequency domain methods discussed above are based on FT. However, wavelet transform (WT), as another versatile candidate in signal processing, has not been studied as much as FT to extract HR using CW Doppler radar. Comparing to other

time–frequency–energy representations, WT has two advantages.

1) It has more options of basis function (mother wavelet), and the mother wavelet can be selected based on the properties of the signal being processed.
2) The basis function of WT is continuous (infinite in time domain but with the energy concentrated in the finite time region), so that WT does not have any window effect introduced by the basis function which exists in some other time–frequency representations such as short-time FT.

Applying WT to the HR extraction using CW Doppler radar, only studies on accurate detection of HR and HR extraction with body motions were reported in [19]–[23]. Tariq and Shiraz [19], Tariq and Ghafouri-Shiraz [20], and Sekine and Maeno [21] focused on the accurate detection of HR. Tariq and Shiraz [19], and Tariq and Ghafouri-Shiraz [20] found the HR by searching the second largest peak on the frequency spectrum. Sekine and Maeno [21] determined the HR by finding the periodicity of Doppler frequencies that depend on heartbeat signal. Tomii and Ohtsuki [22], and Mogi and Ohtsuki [23] proposed methods to detect HR with body motions. These methods search for the scale factor interval that has the wavelet coefficient varying in response to heartbeat during learning and then select a certain scale factor in the interval. During test, the peaks of heartbeat signal are detected using this scale.

Obviously, none of the aforementioned methods addresses the harmonic and fast acquisition issues discussed before. As a result, the study of WT-based algorithm, which is immune to harmonic interferences caused by all sources discussed above and is able to realize fast acquisition of HR using CW Doppler radar, becomes an interest.

In this paper, we introduce a WT-based technique to solve the harmonic issue and to realize the fast acquisition of HR using CW Doppler radar. The proposed data-length-variation technique utilizes the combined wavelet frequency spectrum. It combines the spectrums of a set of 3–5-s data with a length varied in the range of ± 0.5 s. By examining the property of peaks in the spectrum, harmonics can be distinguished from the heartbeat signal. Because, with this technique, the peaks with invariant frequency represent HR, and those with changeable frequency represent harmonics. The proposed method is verified by simulations using numerical computing tool and by experimental tests on human subjects utilizing a 5.8-GHz CW Doppler radar. The measurement results are also analyzed using traditional FT for comparison, and the error is evaluated against the reference from fingertip sensor.

II. Methods

A. Doppler Radar

In CW Doppler radar, the unmodulated transmission signal can be described as follows:

$$T(t) = \cos[2\pi f t + \varphi(t)] \tag{1}$$

where f is the carrier frequency, t is the elapsed time, and $\varphi(t)$ is the phase noise. After being reflected off a target positioned at a distance d_0 with time-varying displacements (chest-wall movements) given by $x(t)$, the received signal can be expressed as follows:

$$R(x) = \cos\left[2\pi f t - \frac{4\pi d_0}{\lambda} - \frac{4\pi x(t)}{\lambda} + \varphi\left(t - \frac{2d_0}{c}\right)\right]. \tag{2}$$

After mixing with the reference signal (transmitted signal) in receiver, the resulting I- and Q-channel baseband signals are

$$B_I(t) = \cos\left[\frac{4\pi x(t)}{\lambda} + \theta + \Delta\varphi\right] \tag{3a}$$

$$B_Q(t) = \sin\left[\frac{4\pi x(t)}{\lambda} + \theta + \Delta\varphi\right] \tag{3b}$$

where $\theta = ((4\pi d_0)/(\lambda))$ is the constant phase shift dependent on the nominal distance to the target d_0, and $\Delta\varphi = \varphi(t) - \varphi(t - ((2d_0)/(c))$ is the residual phase noise. The complex signal is software reconstructed in real time as follows:

$$S(t) = B_I(t) + j * B_Q(t) = \exp\left\{j\left[\frac{4\pi x_r(t)}{\lambda} + \frac{4\pi x_h(t)}{\lambda} + \varphi\right]\right\} \tag{4}$$

where $x_r(t) = m_r sin(\omega_r t + \varphi_r)$ and $x_h(t) = m_h sin(\omega_h t + \varphi_h)$ are periodic chest-wall movements due to respiration and heartbeat, respectively. The CSD eliminates the optimum/null detection point problem by combining I and Q signals in baseband and does not need the calibration of dc offset; therefore, it can measure the vital signs at an arbitrary distance within the detection range. But CSD generates harmonics which may decrease the accuracy of HR detection. The technique in this paper is developed for CSD and can solve the harmonic issue.

B. Wavelet Transform

A general WT is calculated using the following equation:

$$\mathrm{WT}f(a,b) = \frac{1}{\sqrt{a}} \int_{-\infty}^{+\infty} f(t) \Psi^* \left(\frac{t-b}{a}\right) dt \tag{5}$$

where $f(t)$ is the time-series signal being processed, $a (a > 0)$ is a scaling factor, b is a shift factor, and $\Psi((t-b)/(a))$ is the daughter wavelet which is a scaled and shifted version of the mother wavelet $\Psi(t)$. The basic idea behind the WT is that the mother wavelet is scaled by a relating to frequency and shifted along $f(t)$ depending on b to form a daughter wavelet $\Psi((t-b)/(a))$, and then the similarity of daughter wavelet to $f(t)$ is computed and recorded in the WT coefficient WT $f(a,b)$. By repeating the above steps for all b and a until the whole time-series signal and frequencies of interest are covered, we can obtain a coefficient matrix. This approach not only provides the spectral information through scaling, but also preserves the time domain information via shifting the wavelet across the signal. Although we can directly assess the coefficient with respect to variables a and b by plotting the transform results in 3-D, it is inconvenient for quantitative analysis in some cases. In [24], three spectra methods were derived from WT for data analysis and named as wavelet frequency spectrum, point frequency spectrum, and time–frequency spectrum. Wavelet frequency spectrum is established by summing the absolute values of coefficients of

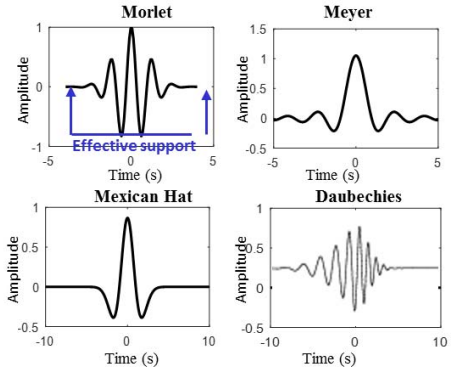

Fig. 1. Examples of commonly used wavelets.

all shift factors on a scale, so the x-axis is the frequency and y-axis is the summed absolute value of the coefficients. This can be depicted as follows:

$$\mathrm{WT}f(a) = \frac{1}{\sqrt{a}} \int_{b_1}^{b_2} |\mathrm{WT}f(a,b)| db. \tag{6}$$

Obviously, wavelet frequency spectrum loses the time information. However, the combined wavelet frequency spectrum proposed in this paper plots the wavelet frequency spectrums of data with a slightly different length on the same figure to address time information of signal.

C. Data-Length-Variation Technique

The proposed data-length-variation technique for fast extraction of HR from the Doppler radar baseband signal utilizes the unique features of the invariant frequency of peak WT coefficient to find HR and changeable frequency of peak WT coefficient to recognize harmonics in the combined wavelet frequency spectrum, while varying a 3–5-s data length. This section is organized by the selection of mother wavelet, long-data-length scenario which applies to the HR extraction, short-data-length scenario which applies to the recognition of harmonics, and the description of the proposed data-length-variation technique.

Unlike FT, WT has a lot of options of basis function, which is called mother wavelet and should be selected based on the properties of signal being processed. Fig. 1 shows four commonly used wavelets. In the proposed technique, the Morlet wavelet, which is defined as $e^{-x^2/2}\cos(5x)$, is chosen as the mother wavelet for three reasons. First, its shape resembles the heartbeat signal from a Doppler radar, so the physical meaning of a peak coefficient from $\Psi((t-b)/(a))$ is an HR at the frequency corresponding to a and at time location b. Second, the single frequency component of the Morlet wavelet ensures the accuracy of extracted HR by translating scale a to pseudo-frequency by $((f_c * f_s)/(a)$, where f_c is the center frequency of the mother wavelet, and it is defined as the frequency at which FT coefficient reaches its peak, and f_s is the sampling rate. The FT of the Morlet wavelet is shown in (7), and the center frequency of the Morlet wavelet is $5/2/\pi = 0.8$ Hz

$$\mathrm{FT}(\Psi(t)) = 1/2\left(e^{-\frac{1}{2}(\omega-5)^2} + e^{-\frac{1}{2}(\omega+5)^2}\right). \tag{7}$$

The third reason is due to its effective support. The effective support is an interval where most energy is confined or where the function is not always close to 0. As shown in Fig. 1, the effective support of the Morlet wavelet is $[-4, 4]$, which corresponds to about 4–5 cycles of a sinusoidal signal with its amplitude shaped by the Gaussian window. The effect of this effective support is the change of upper and lower limits of the integral. WT follows (8) if the length of $f(t)$ is longer than $8a$, which is the integral interval length of WT and the effective support of daughter wavelet. The time duration of 4–5 cycles of a heartbeat is around 4 s, depending on HR, which would fall into the target data length of 3–5 s

$$\mathrm{WT}f(a,b) = \frac{1}{\sqrt{a}} \int_{(-4+b)*a}^{(4+b)*a} f(t)\Psi^*\left(\frac{t-b}{a}\right) dt. \tag{8}$$

Two cases regarding relative data length to the effective support of the corresponding daughter wavelet will be discussed for assisting in introducing the proposed method: long- and short-data-length scenarios. Long-data-length scenario is defined when data contains more than four cycles of signal which is longer than the effective support of the daughter wavelet, and WT follows (8). Short-data-length scenario is defined when data contains less than four cycles of signal which is shorter than the effective support of the daughter wavelet, and WT follows (9).

For the long-data-length scenario, the frequencies of coefficient peaks should be invariant in the combined wavelet frequency spectrum while changing the data length. Because the time duration of the signal is longer than the effective support of the corresponding daughter wavelet, and therefore the daughter wavelet does not "see" the truncations (the beginning and the end) of the signal but the same signal (in frequency domain) even though the data length varies. This feature (stable peaks) of the combined wavelet frequency spectrum will be utilized in the proposed method to determine HR. The numerical simulation in Fig. 2 illustrates this feature by processing a 1.2-Hz sinusoidal signal with a length of 5 s. As shown in Fig. 2(a), the 5-s data contains six cycles of signal and is longer than the effective support of the daughter wavelet. All peaks in the combined wavelet frequency spectrum are at 1.2 Hz while the data length changes from 4 to 5 s, as shown in Fig. 2(b).

For the short-data-length scenario, since the data length is shorter than the effective support $8a$, WT equation turns into

$$\mathrm{WT}f(a,b) = \frac{1}{\sqrt{a}} \int_{t_1}^{t_2} f(t)\Psi^*\left(\frac{t-b}{a}\right) dt \tag{9}$$

where $[t_1, t_2]$ is the time span of the signal under analysis. The effect of this shortened data is the shift of coefficient peaks in the combined wavelet frequency spectrum while varying the data length. Because frequency components introduced by the discontinuities are different if data is truncated at a different position, and the daughter wavelet actually "sees" a different signal as the data length varies. The feature of changing the peak position will be utilized to distinguish the respiratory harmonics from heartbeat signal, which ensures accurate HR extraction when respiratory harmonics are strong. It is worth mentioning that this technique is able to

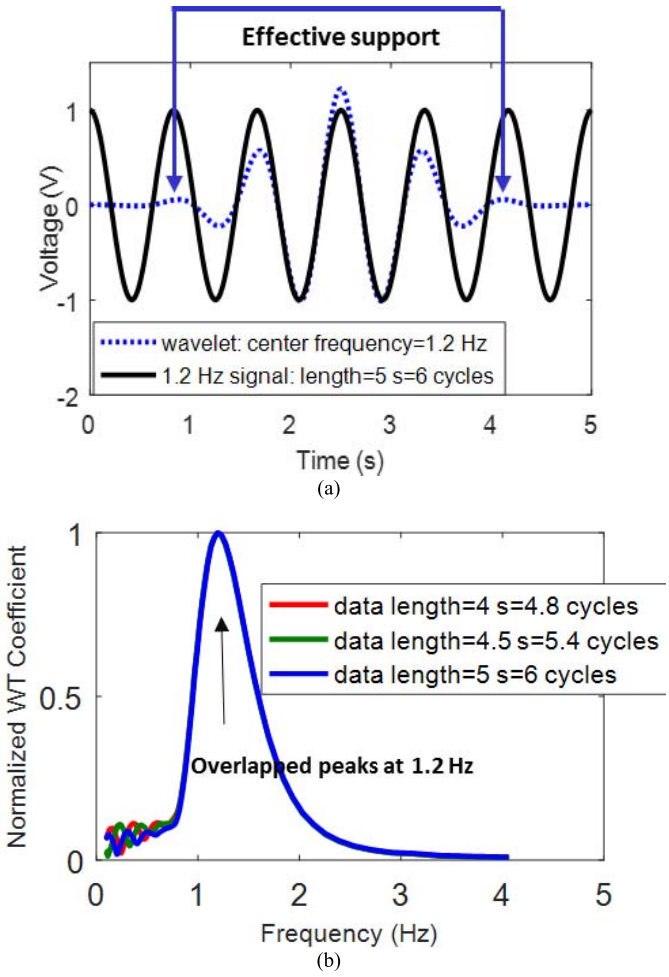

Fig. 2. Long-data-length scenario: the data length is longer than the effective support of the wavelet corresponding to the signal under analysis. (a) Illustration of signal and wavelet. (b) Combined wavelet frequency spectrum of different data lengths.

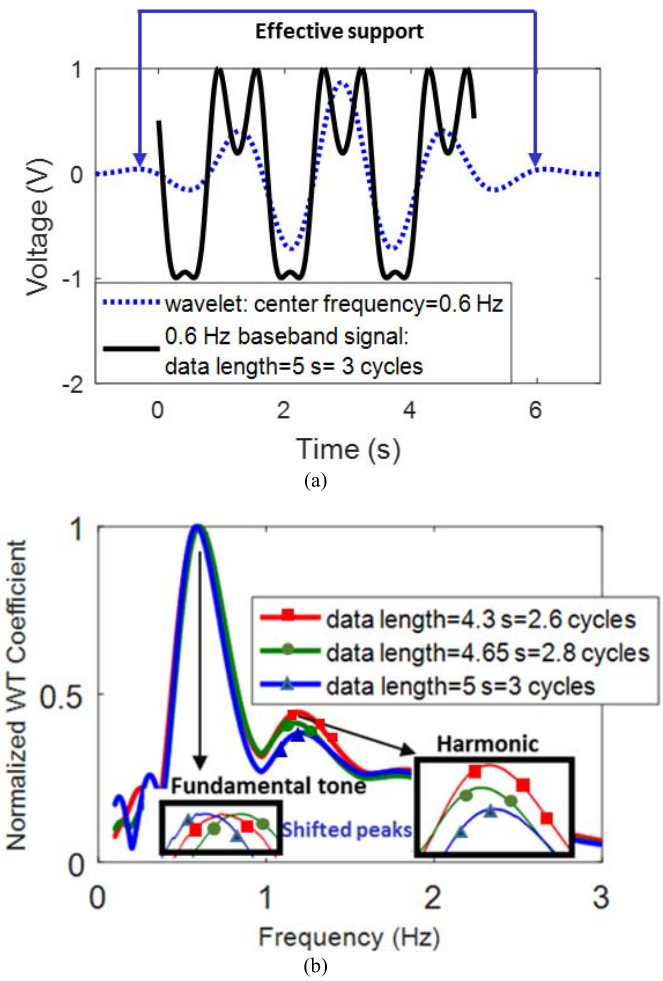

Fig. 3. Short-data-length scenario: the data length is shorter than the effective support of the wavelet corresponding to the signal under analysis. (a) Illustration of signal and wavelet. (b) Combined wavelet frequency spectrum of different data lengths.

deal with the harmonics from a nonsinusoidal respiratory movement as well. Because in the typical range of respiratory rate, both respiratory and harmonic signals apply to the short-data-length scenario. The numerical simulation in Fig. 3 illustrates the above analysis using the baseband signal from the Doppler radar, where the chest-wall movements only contain the 0.6-Hz respiration signal. As shown in Fig. 3(a), 5-s data contains only three cycles of the signal and is shorter than the effective support of the daughter wavelet, so the peaks of fundamental tone and harmonics appear at different frequencies for 4.3-, 4.65-, and 5-s data as shown in Fig. 3(b).

The proposed method selects the data length between the effective support of the daughter wavelet for heartbeat and that for respiration. As a result, the respiration signal is truncated and has discontinuities, while the heartbeat signal can fully be recovered. Therefore, by slightly varying the data length, frequencies of respiration peaks and wavelet harmonics would change while the frequencies of heartbeat peaks are fixed assuming that the HR is constant within a short-time period. It should be noted that the wavelet harmonic is defined as the combination of the respiratory harmonic of Doppler radar baseband signal and the frequency components introduced by the discontinuities of data, so the wavelet harmonic is not necessarily a multiple integer of the fundamental tone.

To illustrate the proposed data-length-variation technique, a simulated signal containing both respiration and heartbeat information is employed to mimic the baseband signal received by a Doppler radar. The signal follows (3) and (4) and the rates of respiration and heartbeat are set to 0.25 and 1.2 Hz, respectively. Fig. 4(a) shows the time domain waveform of both I and Q channels. Fig. 4(b) shows the combined wavelet frequency spectrum of the proposed technique. The data length is varied from 4.2 to 4.8 s with a step of 0.2 s. It can be noted that the peaks with largest amplitudes, representing respiratory rate, alter their corresponding frequencies while varying the data length, and the same is observed for harmonics. In contrast, the frequencies of peaks which represent HR remain the same at 1.2 Hz, as shown by dotted red, green, and blue curves. It is worth mentioning that the behavior of the baseband signal's peaks appearing in the typical HR range is more complicated than that in the example described in the long-data-length scenario. In the example of long-data-length scenario, there is only one frequency component which mimics a heartbeat signal, so all peaks would show at the same frequency while

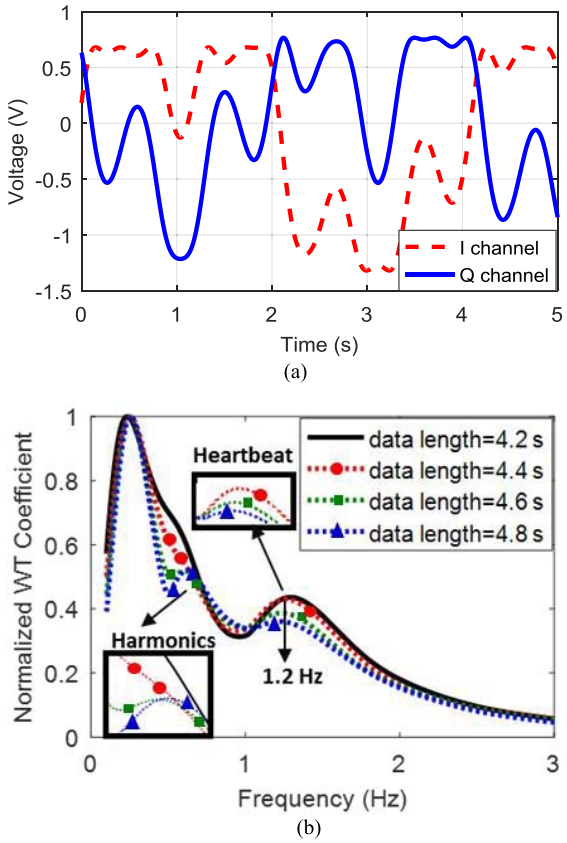

Fig. 4. Analysis of the simulated baseband signal with a 1.2-Hz HR. (a) Time domain waveform of baseband signal of Doppler radar. (b) Combined wavelet frequency spectrum of different data lengths.

varying the data length. However, on the spectrum of the baseband signal from a Doppler radar, in addition to a heartbeat signal, respiratory harmonics, intermodulation products, and frequency components introduced by discontinuities are all possibly appear in the HR range. Moreover, these frequency components may jointly appear as one peak close to the real HR. In this case, the peak might be shifted away from the real HR for some data lengths as represented by the black curve in Fig. 4(b). This shifted peak around 1.2 Hz does not represent heartbeat anymore. The peak formed by those frequency components is possible to overlay the HR for a certain data length. As the data length varies, however, the peak should vary its frequency and shift away from the HR. The proposed algorithm determines HR by searching for peaks with the same frequency and would ignore this kind of shifted peaks.

Fig. 5 shows the flowchart of the proposed algorithm. The algorithm starts with the selection of a section of data with M samples. A length of data M/f_s around 3–5 s is a good starting point. It contains less than four cycles of respiration signal and more than four cycles of heartbeat signal considering typical respiratory rate and HR, and therefore, the tolerance of HR and respiratory harmonics to the data-length-variation will be different. Then, the data length is varied by the interval $\Delta t = N/f_s$ and in the range of $[M - nN/f_s, M + nN/f_s]$. It is reasonable to assume that

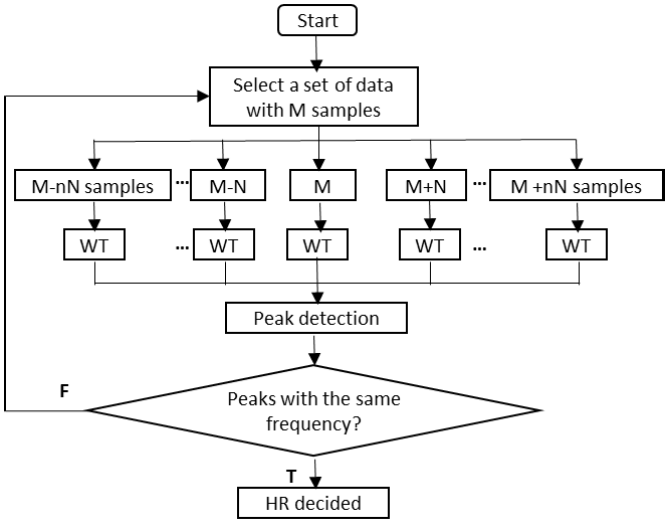

Fig. 5. Flowchart of the proposed data-length-variation technique.

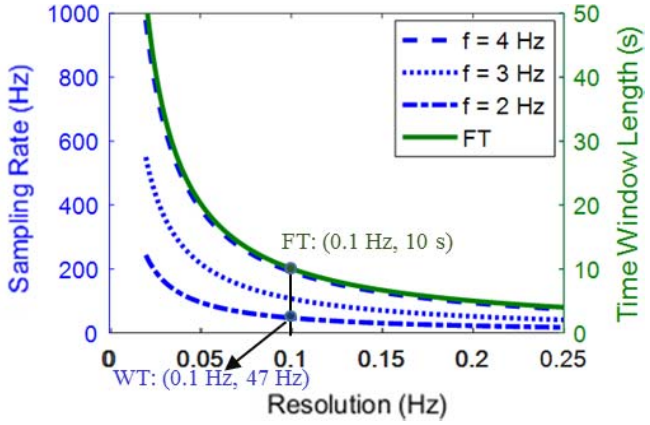

Fig. 6. Resolution comparison between FT and WT.

HR does not change within a short period of time, so the time span of variation $2\Delta t$ is controlled to be shorter than 1 s. The number of data length n can be adjusted around 10 based on the experience from the simulation and experimental data analysis. After that, the wavelet frequency spectrum of each data set is computed. The HR can be determined if several peaks with the same frequency can be detected. If no peak with the same frequency can be detected, the analysis will be repeated by adjusting the data length.

D. Frequency Resolution Analysis

Sufficient frequency resolution is the basis for accurate HR extraction. FT's frequency resolution is inversely proportional to the length of time window. WT has multiresolution with better resolution in lower frequency. We define the resolution R as the difference between two adjacent frequencies as in (12). The resolution is a function of frequency of interest f and sampling rate f_s. Equation (10) can be expressed as (11) where f_s is a function of f and R. Considering a frequency of 2 Hz, f_s is inversely proportional to R as in (11b). Fig. 6 compares the frequency resolution of FT and WT at

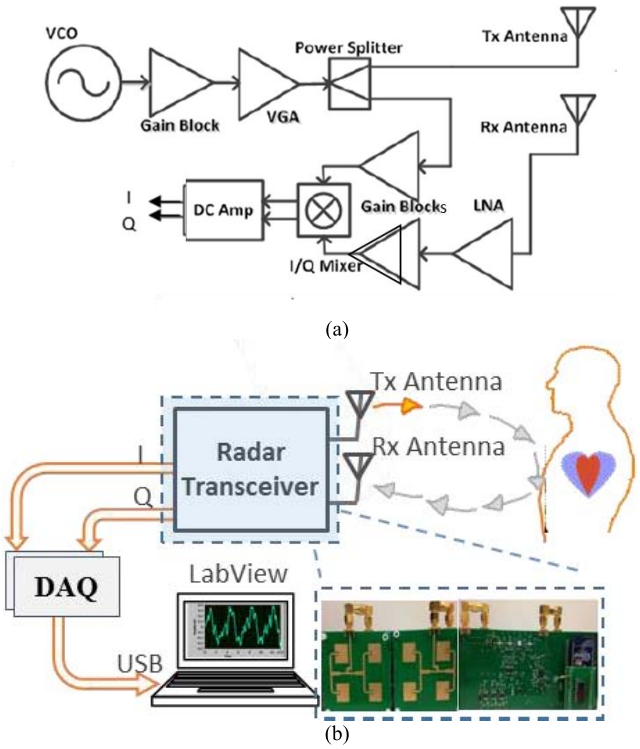

Fig. 7. (a) Architecture of radar transceiver. (b) Illustration of experimental setup of vital signs measurement using Doppler radar.

frequencies of 2, 3, and 4 Hz considering that HR is mostly below 2 Hz. Using WT, to get a resolution better than 0.1 Hz (comparable to a 10-s time window for FT) for frequencies lower than 2 Hz, a sampling rate of 47 Hz is needed

$$R = f(a) - f(a+1) = f\left(1 - \frac{f_s * f_c}{f_s * f_c + f}\right) \quad (10)$$

$$f_s(f, R) = \frac{f^2/f_c}{R} - \frac{f}{f_c} \quad (11a)$$

$$f_s(2, R) = \frac{4.9}{R} - 2.5. \quad (11b)$$

III. Experiments

A. Experimental Setup

In order to verify the proposed technique, a board level 5.8-GHz Doppler radar is developed for experiments. We choose the carrier frequency at 5.8 GHz for two reasons. First, the quarter wavelength of a 5.8-GHz carrier is comparable to the amplitude of human's respiration; thus, the baseband output will not be severely folded. Using lower carrier frequency can increase the approximate linear modulation region, but the antennas' dimensions would be larger. Although the size of antennas would be smaller when employing higher-frequency carrier, the system will consume more power due to higher free space path loss. Thus, 5.8 GHz is a compromise of baseband signal quality, system's physical size, and power consumption. Second, 5.8 GHz is one of the industrial scientific medical bands.

As shown in Fig. 7(a), the radar transceiver employs the homodyne architecture. A sinusoidal signal generated from the voltage-controlled oscillator (HMC 431LP4) is amplified by a gain block (HMC788LP2E) and a variable gain amplifier (VGA, HMC625LP5) on the transmitter (Tx) side. The VGA controls the transmitted power to avoid signal saturation in baseband when detecting a target with very large respiration amplitude, especially when the subject is close to radar. Half of the power from the gain block is transmitted by the Tx antenna, and the other half goes into the LO port of the I/Q mixer (HMC525LC4) for self-mixing to cancel the phase noise utilizing the range correlation effect [18]. The receiver (Rx) consists of a low noise amplifier (HMC318MS8G), two gain blocks (NBB-400), and the I/Q mixer which is used to generate I/Q signal. The reflected signal received by the Rx antenna is directly down-converted to baseband by the I/Q mixer. The baseband quadrature signals are sampled by an A/D converter, and then the data is transferred to a computer for processing. Fig. 7(b) shows the experimental setup diagram.

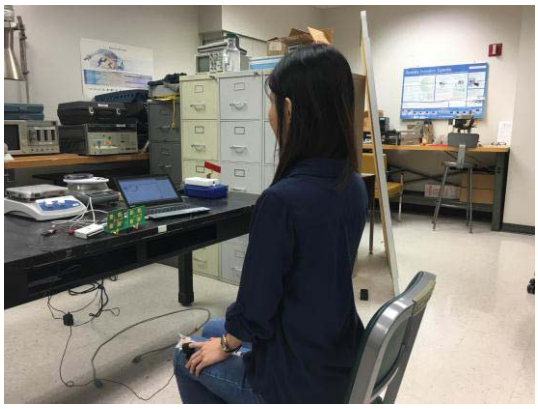

Fig. 8. Photograph of experimental setup in laboratory environment.

Tests were performed in the laboratory environment shown in Fig. 8. The subject sat in front of the radar within the normal detection range, and was breathing normally. A wired finger-pressure pulse sensor UFI_1010 was attached to the index finger to measure the pulse rate simultaneously, which was used as the reference for HR.

B. Experimental Results and Analysis

For the signal processing of a series of L-s data using the proposed data-length-variation technique, the length L was arbitrarily selected in the range of 3–5 s, and then the selected data length was varied with a step of 0.1 s in the range of ± 0.5 s to obtain ten data sets. By detecting peaks with the same frequency in the combined wavelet frequency spectrum of the ten data sets, HR was determined. To obtain the reference for each series of data, the fingertip sensor signal was averaged within $(L + 0.5)$ s. For comparison, data were also processed using the traditional FT (length of time window is $(L + 0.5)$ s) followed by searching the second highest peak in the spectrum. The comparison shows how much the accuracy can be improved by successfully recognizing the harmonics using the proposed algorithm. Fig. 9 shows the information of one set of 5-s data. It is difficult to directly extract HR from the time domain data, as shown in Fig. 9(a). The fingertip sensor

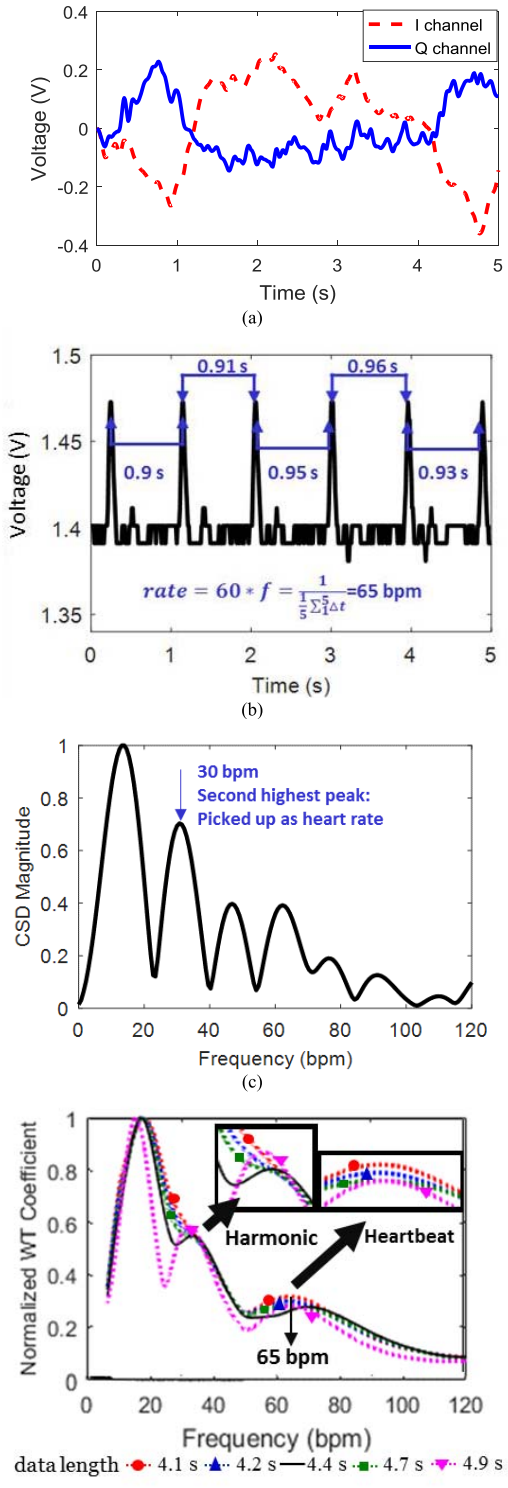

Fig. 9. Information of one set of 5-s data. (a) Time domain waveform. (b) 5-s data of fingertip sensor, extracted average rate is used as the reference. (c) Fourier frequency spectrum of 5-s data. (d) Combined wavelet frequency spectrum using the proposed data-length-variation technique.

data in Fig. 9(b) result in an HR of 65 bpm. The Fourier spectrum in Fig. 9(c) shows the second highest peak at 30 bpm, which is picked as the HR but is actually the respiratory harmonic. However, the combined wavelet frequency spectrum

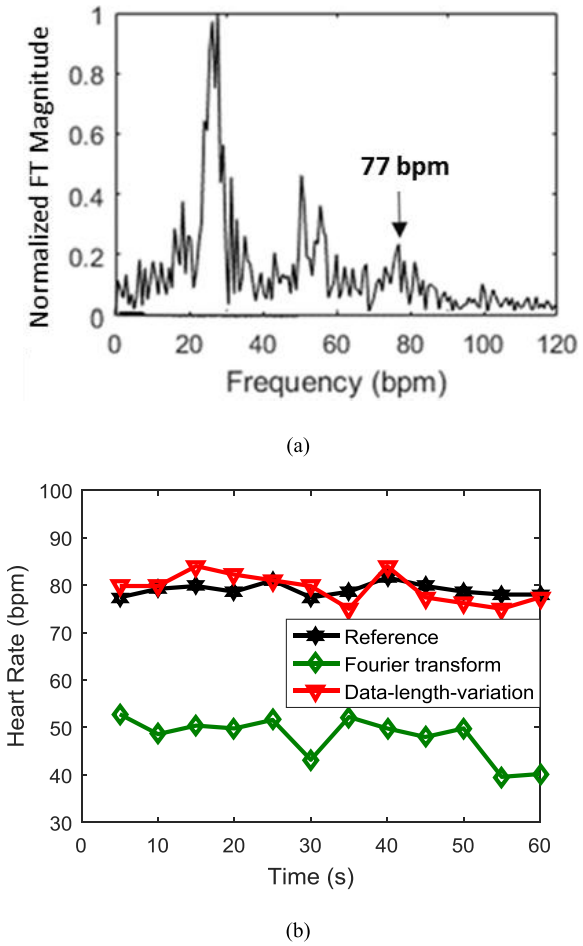

Fig. 10. Measurement A: HR versus time obtained with different measurement methods. For all 5-s data sections, respiratory harmonics are stronger than heartbeat signal. (a) Fourier spectrum of 60-s data. (b) Postprocessing results of HR extracted from FT of 5-s data and from the data-length-variation technique using a 4.5-s data length which is varied in the range of ±0.5 s. The rates from fingertip sensor are averaged across each 5-s data section, and the average is used as the reference.

in Fig. 9(d) (for concise illustration, only five traces are shown) using the proposed technique shows peaks with the same frequency at 65 bpm which represents HR and is the same as the reference. The peak with the frequency of 75 bpm on the black curve does not represent heartbeat due to the same reason discussed for Fig. 4(b). It is worth noting that this kind of shifted peak may happen at an arbitrary data length. The algorithm searches for peaks with the same frequency which represents HR and would ignore this kind of shifted peaks. The analysis will be repeated by adjusting the data length if no peak with the same frequency can be detected.

Figs. 10 and 11 show the results of two 60-s measurements which were taken from two subjects. Measurement A was performed under the condition that the subject always breathed deeply. Fig. 10(a) shows the Fourier spectrum of the whole 60-s data set. It can be seen that the respiratory harmonics have larger magnitudes than heartbeat. Thus, the HR obtained with the traditional FT would be around 50 bpm, which is actually the frequency of respiratory harmonic but extracted as the HR

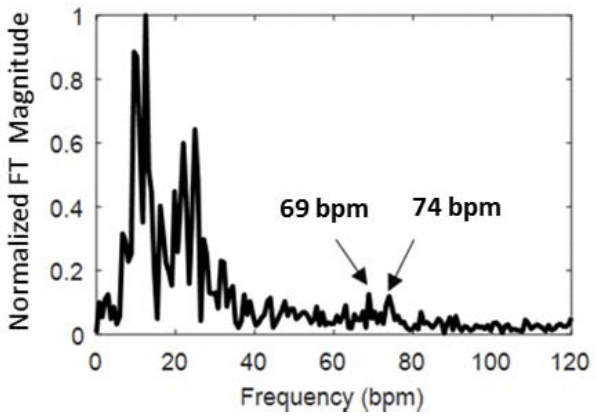

(a)

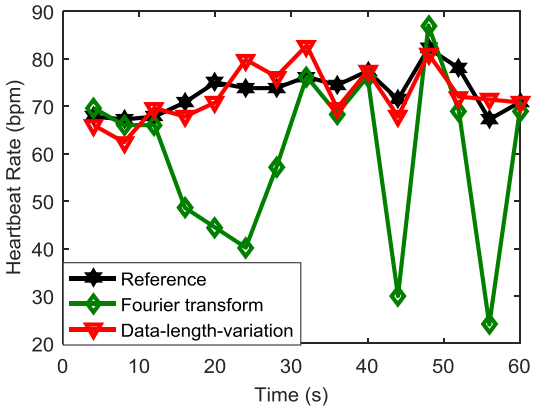

(b)

Fig. 11. Measurement B: HR versus time obtained with different measurement methods. For a different 4-s data set, respiratory harmonic may be stronger or weaker than heartbeat signal. (a) Fourier spectrum of 60-s data. (b) Postprocessing results of HR extracted from FT of 4-s data and from the data-length-variation technique using a 3.5-s data length which is varied in the range of ±0.5 s. The rates from fingertip sensor are averaged across each 4-s data section, and the average is used as the reference.

incorrectly. However, the proposed method using a 4.5-s data length is able to extract the correct HR as shown in Fig. 10(b). Fig. 11 shows the results obtained with measurement B, in which the subject intentionally had deep and shallow breath alternately to create the scenario that respiratory harmonic was strong and weak alternately. Fig. 11(a) shows the Fourier spectrum of the whole 60-s data set, it has strong respiratory harmonics and has two heartbeat peaks at 67 and 71 bpm which indicates the change of the HR. It is worth noting that FT works well when harmonic is weaker than heartbeat signal and fails when harmonic is stronger than heartbeat signal, as shown in Fig. 11(b). In contrast, the results obtained by the proposed method using a 3.5-s data length follow the reference very well regardless of the strength of harmonics.

The average error was used to quantify the accuracy of different methods, which was defined as

$$\text{error} = \frac{1}{N}\sum_{1}^{N}\frac{|\text{HR}_{\text{ref}} - \text{HR}_{\text{meas}}|}{\text{HR}_{\text{ref}}} \tag{12}$$

TABLE I
COMPARISON OF HR MEASUREMENT ERRORS WITH DIFFERENT METHODS

Measurement	A (always w/ strong harmonics)	B (w/ alternately strong and weak harmonics)	C (no specific characteristic)	Average
FT	39%	21%	20%	26.7%
WT-based data-length-variation technique	3%	4.6%	3%	3.5%

where N is the number of data sets, HR_{ref} is the average HR from the fingertip sensor, and HR_{meas} is the HR of measurement. Table I summarizes the error of measurements A and B with different methods. The error of an additional measurement C is also listed. Compared to the traditional frequency domain method using FT, the proposed technique reduces the average error of HR from 39% to 3% (measurement A), from 21% to 4.6% (measurement B), and from 25% to 3% (measurement C). The average error of the three measurements is reduced from 26.7% to 3.5%.

In summary, the proposed data-length-variation technique achieves the fast HR extraction with only a 3–5-s data length and good accuracy by successfully recognizing respiratory harmonics.

IV. Conclusion

In this paper, a WT-based data-length-variation technique is proposed to realize fast detection (only requiring a 3–5 s data length) of HR utilizing CW Doppler radar. Compared to the traditional FT method, the accuracy is improved dramatically, because the proposed method is able to distinguish respiratory harmonics from the heartbeat signal by examining the peak property of the combined wavelet frequency spectrum. The algorithm is elaborated and demonstrated by numerical simulations, in conjunction with controlled laboratory experiments. The proposed method achieves an average HR error of 3.5% using a 3–5-s data length varied with a step of 0.1 s in the range of ±0.5 s for the signal processing.

Compared to the state-space method in [17], which uses 12-s data and achieves less than 3% error, and to the Fourier-transform-based time-window-variation technique in [16], which uses a 2–5-s time window and obtains less than 5% error, the work in this paper achieves comparable accuracy with 3–5-s data by using WT-based data-length-variation technique.

References

[1] J. C. Lin, "Noninvasive microwave measurement of respiration," *Proc. IEEE*, vol. 63, no. 10, p. 1530, Oct. 1975.
[2] J. C. Lin and J. Salinger, "Microwave measurement of respiration," in *IEEE MTT-S Int. Microw. Symp. Dig.*, May 1975, pp. 285–287.
[3] J. C. Lin, J. Kiernicki, M. Kiernicki, and P. B. Wollschlaeger, "Microwave apexcardiography," *IEEE Trans. Microw. Theory Techn.*, vol. MTT-27, no. 6, pp. 618–620, Jun. 1979.
[4] C. Li, J. Lin, and Y. Xiao, "Robust overnight monitoring of human vital signs by a non-contact respiration and heartbeat detector," in *Proc. 28th Annu. Int. Conf. IEEE Eng. Med. Biol. Soc.*, Aug./Sep. 2006, pp. 2235–2238.
[5] K.-M. Chen, Y. Huang, J. Zhang, and A. Norman, "Microwave life-detection systems for searching human subjects under earthquake rubble or behind barrier," *IEEE Trans. Biomed. Eng.*, vol. 47, no. 1, pp. 105–114, Jan. 2000.

[6] A. Singh, S. S. Lee, M. Butler, and V. Lubecke, "Activity monitoring and motion classification of the lizard Chamaeleo jacksonii using multiple Doppler radars," in *Proc. Annu. Int. Conf. IEEE Eng. Med. Biol. Soc.*, Aug./Sep. 2012, pp. 4525–4528.

[7] T.-Y. Huang, J. Lin, and L. Hayward, "Non-invasive measurement of laboratory rat's cardiorespiratory movement using a 60-GHz radar and nonlinear Doppler phase modulation," in *Proc. IEEE MTT Int. Micro Workshop Ser. RF Wireless Technol. Biomed. Healthcare Appl.*, Sep. 2015, pp. 83–84.

[8] A. D. Droitcour, O. Boric-Lubecke, V. M. Lubecke, and J. Lin, "0.25 μm CMOS and BiCMOS single-chip direct-conversion Doppler radars for remote sensing of vital signs," in *IEEE Int. Solid-State Circuits Conf. (ISSCC) Dig. Tech. Papers*, Feb. 2002, pp. 348–349.

[9] M. Chen, O. Boric-Lubecke, and V. M. Lubecke, "0.5-μm CMOS implementation of analog heart-rate extraction with a robust peak detector," *IEEE Trans. Instrum. Meas.*, vol. 57, no. 4, pp. 690–698, Apr. 2008.

[10] S. Bakhtiari *et al.*, "Compact millimeter-wave sensor for remote monitoring of vital signs," *IEEE Trans. Instrum. Meas.*, vol. 61, no. 3, pp. 830–841, Mar. 2012.

[11] J. Kranjec, S. Beguš, J. Drnovšek, and G. Geršak, "Novel methods for noncontact heart rate measurement: A feasibility study," *IEEE Trans. Instrum. Meas.*, vol. 63, no. 4, pp. 838–847, Apr. 2014.

[12] M. Singh and G. Ramachandran, "Reconstruction of sequential cardiac in-plane displacement patterns on the chest wall by laser speckle interferometry," *IEEE Trans. Biomed. Eng.*, vol. 38, no. 5, pp. 483–489, May 1991.

[13] B.-K. Park, O. Boric-Lubecke, and V. M. Lubecke, "Arctangent demodulation with DC offset compensation in quadrature Doppler radar receiver systems," *IEEE Trans. Microw. Theory Techn.*, vol. 55, no. 5, pp. 1073–1079, May 2007.

[14] C. Li and J. Lin, "Complex signal demodulation and random body movement cancellation techniques for non-contact vital sign detection," in *IEEE MTT-S Int. Microw. Symp. Dig.*, Jun. 2008, pp. 567–570.

[15] J. Tu and J. Lin, "Respiration harmonics cancellation for accurate heart rate measurement in non-contact vital sign detection," in *IEEE MTT-S Int. Microw. Symp. Dig.*, Jun. 2013, pp. 1–3.

[16] J. Tu and J. Lin, "Fast acquisition of heart rate in noncontact vital sign radar measurement using time-window-variation technique," *IEEE Trans. Instrum. Meas.*, vol. 65, no. 6, pp. 112–122, Dec. 2016.

[17] K. Naishadham, J. E. Piou, L. Ren, and A. E. Fathy, "Estimation of cardiopulmonary parameters from ultra wideband radar measurements using the state space method," *IEEE Trans. Biomed. Circuits Syst.*, vol. 10, no. 6, pp. 1037–1046, Dec. 2016.

[18] A. D. Droitcour, O. Boric-Lubecke, V. M. Lubecke, J. Lin, and G. T. A. Kovacs, "Range correlation and I/Q performance benefits in single-chip silicon Doppler radars for noncontact cardiopulmonary monitoring," *IEEE Trans. Microw. Theory Techn.*, vol. 52, no. 3, pp. 838–848, Mar. 2004.

[19] A. Tariq and H. Shiraz, "Doppler radar vital signs monitoring using wavelet transform," in *Proc. Antennas Propag. Conf.*, Nov. 2010, pp. 293–296.

[20] A. Tariq and H. Ghafouri-Shiraz, "Vital signs detection using Doppler radar and continuous wavelet transform," in *Proc. 5th Eur. Conf. Antennas Propag. (EUCAP)*, Apr. 2011, pp. 285–288.

[21] M. Sekine and K. Maeno, "Non-contact heart rate detection using periodic variation in Doppler frequency," in *Proc. IEEE Sensors Appl. Symp.*, Feb. 2011, pp. 318–322.

[22] S. Tomii and T. Ohtsuki, "Heartbeat detection by using Doppler radar with wavelet transform based on scale factor learning," in *Proc. IEEE Int. Conf. Commun.*, Jun. 2015, pp. 483–488.

[23] E. Mogi and T. Ohtsuki, "Heartbeat detection with Doppler sensor using adaptive scale factor selection on learning," in *Proc. IEEE 26th Annu. Int. Symp. Pers., Indoor, Mobile Radio Commun.*, Aug. 2015, pp. 2166–2170.

[24] X. Lu, H. Liu, J. Kang, and J. Cheng, "Wavelet frequency spectrum and its application in analyzing an oscillating chemical system," *Anal. Chim. Acta*, vol. 484, no. 2, pp. 201–210, May 2003.

Meiyu Li received the B.S. degree in optoelectronic and information engineering from the Harbin Institute of Technology, Harbin, China, in 2009, and the master's degree in electrical and computer engineering from the University of Florida, Gainesville, FL, USA, in 2013.

Her current research interests include the Doppler radar system and measurement algorithms for noncontact vital sign detection on human.

Jenshan Lin (S'91–M'94–SM'00–F'10) received the Ph.D. degree in electrical engineering from the University of California at Los Angeles (UCLA), Los Angeles, CA, USA, in 1994.

From 1994 to 2001, he was with the Lucent Bell Labs, Murray Hill, NJ, USA. From 2001 to 2003, he was with Agere Systems, Allentown, PA, USA, a spin-off company of Lucent Bell Labs. In 2003, he joined the University of Florida, Gainesville, FL, USA, where he is currently a Professor. Since 2016, he has been a Program Director of the Communications, Circuits, and Sensing Systems Program with the U.S. National Science Foundation. He has authored or co-authored over 260 technical publications in refereed journals and conference proceedings and holds 15 U.S. patents. His current research interests include sensors and biomedical applications of microwave and millimeter-wave technologies, wireless power transfer, and wireless communication systems.

Dr. Lin was the General Chair of the 2008 RFIC Symposium, the Technical Program Chair of the 2009 Radio and Wireless Symposium, and the General Co-Chair of the 2012 Asia–Pacific Microwave Conference. He was a recipient of the 1994 UCLA Outstanding Ph.D. Award, the 1997 Eta Kappa Nu Outstanding Young Electrical Engineer Honorable Mention Award, the 2007 IEEE MTT-S N. Walter Cox Award, and the 2015 IEEE Wireless Power Transfer Conference Best Paper Award. He served as an Associate Editor of the IEEE TRANSACTIONS ON MICROWAVE THEORY AND TECHNIQUES from 2006 to 2010, and served as an Editor-in-Chief of the IEEE TRANSACTIONS ON MICROWAVE THEORY AND TECHNIQUES. He serves on the Editorial Advisory Board of the Cambridge University Press "RF and Microwave Engineering Series."